IOSR Journal of Applied Physics (IOSR-JAP)
e-ISSN: 2278-4861.Volume 7, Issue 5 Ver. I (Sep. - Oct. 2015), PP 67-75
www.iosrjournals

Crystal dynamics of zinc chalcogenides II: An application to ZnSe

Jay Prakash Dubey[1*], Raj Kishore Tiwari[2], Kripa Shankar Upadhyaya[3], Pramod Kumar Pandey[1]

[1,*]*Department of Physics, Pandit Sambhoo Nath Shukla Government Post Graduate College, Shahdol "Awadhesh Pratap Singh University", Rewa- 486003, M. P., India*
[2] *Department of Physics, Government New Science College, "Awadhesh Pratap Singh University", Rewa- 486003, M. P., India*
[3] *Department of Physics, Nehru Gram Bharati University, Allahabad- 221505, U. P., India*

Abstract: *A theoretical model to study the dynamical behaviour of zinc blende structure crystals has been formulated. This model is known as van der Waal's three body force rigid shell model (VTRSM). This new model incorporates the effect of van der Waal's interactions and three-body interactions into the rigid shell model of zinc blende structure, where the short range interactions are operative upto the second neighbours. The model thus developed, has been applied to study the phonon dispersion curves (PDCs) along the three principal symmetry directions, Debye temperatures variation, Combined density of states (CDS) curves, two-phonon Raman / IR peaks and anharmonic elastic properties (third order elastic constants and their pressure derivatives) of ZnSe. Our results are in good agreement with the available measured data. It is concluded that this model VTRSM will be equally applicable to study above properties of other zinc blende structure solids as compared to the models of earlier researchers.*

Keywords: *Phonons , van der Waal's interactions , Debye temperatures variation , Combined density of states curve , Raman spectra , zinc selenide , phonon dispersion curves , lattice dynamics.*
PACS No: 63.20.-e, 65.40.Ba, 78.30.-j

I. Introduction

The semiconductors of zinc-blende structure (ZBS) crystals are promising attraction for numerous experimental and theoretical investigations in recent years. These investigations are consequences efforts devoted to understand the interesting crystal properties of phonon dispersion curves, harmonic and anharmonic elastic constants, Debye temperatures variation, combined density of states, cohesive energy, two phonon IR and Raman spectra and numerous other physical properties. In the earlier past, it was an extensive theoretical study of the phase-transition and anharmonic properties of the solids by different type of cohesive energy. The maximum cohesive energy potentials are contributed with long-range Coulomb interactions and short-range overlap repulsion. The overlap repulsion is a sum of lattice to describe the cohesive energy in the most of ionic solids by Born and Mayer [1]. The earlier researchers Tosi and Fumi [2] properly incorporated van der Waal's interaction along dipole-dipole (d-d) and dipole-quadrupole (d-q) interactions respectively to reveal the cohesive energy in several ionic solids. Hafemeister and Flygare [3] followed the three body interactions and overlap repulsion upto second neighbour ions besides short range interactions. We also quote the work of Singh [4], who introduced the effects of charge transfer i.e. despite their successes, the basic nature of these inter atomic potentials i.e. they are inadequate to reveal a consistent picture of the interaction mechanism in ionic solids. The present investigation of van der Waal's three body force rigid shell model (VTRSM) is organized as follows. We begin with the estimation of van der Waal's coefficient from the Slater-Kirkwood variation method [5] with both ions are polarizable. Later on, third order elastic constants and pressure derivatives are deduced within framework of the rigid shell model, that incorporates the long-range Coulomb interactions, van der Waal's (vdW) interactions, the short range overlap repulsive interaction upto second neighbour ions and three-body interactions. The structural properties of IIB-VIA semiconductors have been a subject of much interest both experimentally and theoretically [6-16] due to their polymorphic structure. The second order elastic constants of ZnSe have been determined Berlincourt et al. [17] piezo resonance technique, Lee [18] ultrasonic pulse-echo method, Hennion et al. [19] inelastic neutron scattering, Hodgins [20] brillouin scattering, Kunk et al. [21] rigid ion model, Talwar et al. [22] 11-parameter rigid ion model, Rajput and Browne [23] six-parameter adiabatic charge model has also been quite successful in explaining the phonon spectra, Sharma [24] effective interactional potential model, Wang et al. [25] density functional perturbation theory, Tista Basak et al. [26] ab initio as well as potential model and so on.

In this communication, we have included (i) the effect of VDWI and (ii) TBI in the framework of RSM where short range interactions are effective upto the second neighbours. Our new model VTRSM has 14-parameters i.e. four TBI parameters b, ρ, $f(r_0)$, $r_0 f'(r_0)$; six nearest and the next nearest neighbour short-range

repulsive interaction parameters A_{12}, B_{12}, A_{11}, B_{11}, A_{22}, B_{22} two distortion polarizabilities of negative and positive ions d_1, d_2 and two shell charges of the negative and positive ions Y_1, Y_2 respectively. They can be deduced with the help of measured values of elastic constants, dielectric constants, electronic polarizabilities and van der Waal's coupling coefficients. This model has been applied to study the lattice dynamics of zinc chalcogenides (ZnS, ZnSe, ZnTe). In this paper, we are reporting the study of phonon dispersion curves, Debye temperatures variation, combined density of states (CDS) curves, third order elastic constants and pressure derivatives of SOEC. The formalism of our model has been presented in the next section in detail.

II. Theoretical Framework of the Present Model

We have developed a model for ZBS structure, which includes the effect of van der Waal's interactions (VDWI) and three body interactions (TBI) in the frame work of rigid shell model (RSM) where short range interactions are effective upto the second neighbours and known as van der Waal's three body force rigid shell model (VTRSM).

2.1. Secular Equations

For ZBS crystals, the cohesive energy for a particular lattice separation *(r)* has been expressed as

$$\Phi(r) = \Phi_{LR}(r) + \Phi_{SR}(r) \tag{1}$$

where the first term $\Phi_{LR}(r)$ represents the long-range Coulomb and three body interaction (TBI) energies expressed by

$$\Phi_{LR}(r) = -\sum_{\substack{ij \\ i\neq j\neq k}} \frac{Z_i Z_j e^2}{r_{ij}} \left\{1 + \sum_k f(r_{ik})\right\} = -\frac{\alpha_M Z^2 e^2}{r}\left\{1 + \frac{4}{Z} f(r)\right\} \tag{2}$$

where Z_i is the ionic charge parameter of i^{th} ion, r_{ij} separation between i^{th} and j^{th} ion, $f(r_{ik})$ is the three-body force parameter dependent on nearest-neighbour separation r_{ik} and is a measure of ion size difference Singh [4], α_M is Madelung constant (=1.63805 for ZBS).

The second term in equation (1) is short-range energy contributions from overlap repulsion and van der Waal's interactions (VDWI) expressed as [27].

$$\Phi_{SR}(r) = Nb \sum_{i,j=1}^{2} \beta_{ij}\, exp\left[\frac{r_i + r_j - r_{ij}}{\rho}\right] - \sum_{ij} \frac{c_{ij}}{r_{ij}^6} - \sum_{ij} \frac{d_{ij}}{r_{ij}^8} \tag{3}$$

where *N* is the Avogadro's a number, b is the hardness parameters and the first term is the Hafemeister and Flygare (HF) potential Hafemeister and Flygare [3] and used by Singh and coworkers. The second term and third term represent the energy due to VDW for c_{ij} dipole-dipole (d-d) and d_{ij} dipole-quadrupole (d-q) interactions, respectively.

Using the crystal energy expression (1), the equations of motion of two cores and two shells can be written as;

$$\omega^2 \underline{M}\,\underline{U} = \left(\underline{R} + \underline{Z_m}\,\underline{C'}\,\underline{Z_m}\right)\underline{U} + \left(\underline{T} + \underline{Z_m}\underline{C'}\,\underline{Y_m}\right)\underline{W} \tag{4}$$

$$O = \left(\underline{T}^T + \underline{Y_m}\,\underline{C'}\,\underline{Z_m}\right)\underline{U} + \left(\underline{S} + \underline{K} + \underline{Y_m}\underline{C'}\,\underline{Y_m}\right)\underline{W} \tag{5}$$

Here $\underline{U}$ and $\underline{W}$ are vectors describing the ionic displacements and deformations, respectively. $\underline{Z_m}$ and $\underline{Y_m}$ are diagonal matrices of modified ionic charges and shell charges, respectively; $\underline{M}$ is the mass of the core; $\underline{T}$ and $\underline{R}$ are repulsive Coulombian matrices respectively; $\underline{C'}$ and $\underline{Y_m}$ are long-range interaction matrices that include Coulombian and TBI respectively; $\underline{S}$ and $\underline{K}$ are core-shell and shell-shell repulsive interaction matrices, respectively and $\underline{T}^T$ is the transpose of matrix $\underline{T}$. The elements of matrix $\underline{Z_m}$ consist of the parameter Z_m giving the modified ionic charge.

$$Z_m = \pm Z\sqrt{1 + \left(\frac{8}{Z}\right) f(r_0)} \tag{6}$$

The elimination of $\underline{W}$ from eqns. (4) and (5) leads to the secular determinant;

$$\left|\underline{D}(\vec{q}) - \omega^2 \underline{M}\,\underline{I}\right| = 0 \tag{7}$$

for the frequency determination. Here $\underline{D}$ (q) is the (6×6) dynamical matrix given by

$$\underline{D}(\vec{q}) = \left(\underline{R'} + \underline{Z_m}\underline{C'}\,\underline{Z_m}\right) - \left(\underline{T} + \underline{Z_m}\underline{C'}\,\underline{Y_m}\right) \times \left(\underline{S} + \underline{K} + \underline{Y_m}\underline{C'}\underline{Y_m}\right)^{-1}\left(\underline{T}^T + \underline{Y_m}\,\underline{C'}\,\underline{Z_m}\right) \tag{8}$$

The numbers of adjustable parameters have been largely reduced by considering all the short-range interactions to act only through the shells.

2.2. Vibrational Properties of Zinc-Blende Structure

By solving the secular equation (4) along [q00] direction and subjecting the short and long-range coupling coefficients to the long-wavelength limit $\vec{q} \to 0$ two distinct optical vibration frequencies are obtained as

$$(\mu\omega_L^2)_{q=0} = R_0^{'} + \frac{(Z^{'}e)^2}{vf_L} \cdot \frac{8\pi}{3}(Z_m^2 + 4Zr_0 f^{'}(r_0)) \tag{9}$$

$$(\mu\omega_T^2)_{q=0} = R_0^{'} - \frac{(Z^{'}e)^2}{vf_T} \cdot \frac{4\pi}{3}Z_m^2 \tag{10}$$

where the abbreviations stand for

$$R_0^{'} = R_0 - e^2\left(\frac{d_1^2}{\alpha_1} + \frac{d_2^2}{\alpha_2}\right); R_0 = \frac{e^2}{v}\left[4\ \frac{A_{12}+2B_{12}}{3}\right];\ Z^{'} = Z_m + d_1 - d_2 \tag{11}$$

$$f_L = 1 + \left(\frac{\alpha_1+\alpha_2}{v}\right) \cdot \frac{8\pi}{3}(Z_m^2 + 4Zr_0 f^{'}(r_0)) \tag{12}$$

$$f_T = 1 - \left(\frac{\alpha_1+\alpha_2}{v}\right) \cdot \frac{4\pi}{3} \tag{13}$$

and

$$\alpha = \alpha_1 + \alpha_2 \tag{14}$$

And $v = 3.08r_0^3$ for ZBS (volume of the unit cell).

2.3. Debye Temperatures Variation

The specific heat at constant volume C_v at temperature T is expressed as

$$C_v = 3Nk_B \frac{\int_0^{\upsilon_m}\left\{\left(\frac{h\upsilon}{k_BT}\right)^2 e^{h\upsilon/k_BT}\right\}G(\upsilon)d\upsilon \Big/ \left(e^{h\upsilon/k_BT}-1\right)^2}{\int_0^{\upsilon_m} G(\upsilon)d\upsilon} \tag{15}$$

Where, υ_m is the maximum frequency, h is the Planck's constant and k_B is the Boltzmann's constant. The equation (15) can be written as a suitable form for a computational purpose as

$$C_v = 3Nk_B \frac{\sum_\upsilon \{E(x)\}G(\upsilon)d\upsilon}{\sum_\upsilon G(\upsilon)d\upsilon} \tag{16}$$

where E(x) is the Einstein function, defined by

$$E(x) = x^2 \frac{exp(x)}{\{exp(x)-1\}^2} \tag{17}$$

where $x = \left\{\left(\frac{h\upsilon}{k_BT}\right)^2 e^{\frac{h\upsilon}{k_BT}}\right\}$

Also,

$\sum_\upsilon G(\upsilon)d\upsilon$ = Total number of frequencies considered.

= 6000 for zinc-blende structure.

Hence, equation (16) can be written for zinc-blende structure type crystals, as

$$C_v = \frac{3Nk_B}{6000}\sum_\upsilon E(x)G(\upsilon)d\upsilon \tag{18}$$

The contribution of each interval to the specific heat is obtained by multiplying an Einstein function corresponding to mid-point of each interval (say 0.1 THz) by its statistical weight. The statistical weight of the interval is obtained from the number of frequencies lying in that interval. The contributions of all such intervals when summed up give $\sum_\upsilon E(x)G(\upsilon)d\upsilon$. The Specific heat C_v is then calculated by expression (18).

2.4. Second and Third Order Elastic Constant

Proceeding with the use of three body crystal potential given by equation (1), (Sharma and Verma [28]) have derived the expressions for the second order elastic constants and used by (Singh and Singh [29]) for zinc-blende structure crystals. We are reporting them here as their corrected expressions.

The expressions for second order elastic constants (SOEC) are-

$$C_{11} = L\left[0.2477Z_m^2 + \frac{1}{3}(A_1 + 2B_1) + \frac{1}{2}(A_2 + B_2) + 5.8243Zaf^{'}(r_0)\right] \tag{19}$$

$$C_{12} = L\left[-2.6458Z_m^2 + \frac{1}{3}(A_1 - 4B_1) + \frac{1}{4}(A_2 - 5B_2) + 5.8243Zaf^{'}(r_0)\right] \tag{20}$$

$$C_{44} = L\left[-0.123Z_m^2 + \frac{1}{3}(A_1 + 2B_1) + \frac{1}{4}(A_2 + 3B_2) - \frac{1}{3}\nabla(-7.539122Z_m^2) + A_1 - B_1\right] \tag{21}$$

where $A_1 = A_{12}$, $B_1 = B_{12}$, $A_2 = A_{11} + A_{22}$, $B_2 = B_{11} + B_{22}$, $C_1 = \frac{A_{12}^2}{B_{12}}$ and $C_2 = \frac{A_2^2}{B_2}$

and the expressions for third order elastic constants (TOEC) are-

$$C_{111} = L\left[0.5184Z_m^2 + \frac{1}{9}(C_1 - 6B_1 - 3A_1) + \frac{1}{4}(C_2 - B_2 - 3A_2) - 2(B_1 + B_2) - 9.9326Zaf'(r_0) + 2.5220Za^2f\,"(r_0)\right] \quad (22)$$

$$C_{112} = L\left[0.3828Z_m^2 + \frac{1}{9}(C_1 + 3B_1 - 3A_1) + \frac{1}{8}(C_2 + 3B_2 - 3A_2) - 11.642Zaf'(r_0) + 2.5220Za^2f\,"(r_0)\right] \quad (23)$$

$$C_{123} = L\left[6.1585Z_m^2 + \frac{1}{9}(C_1 + 3B_1 - 3A_1) - 12.5060Zaf'(r_0) + 2.5220Za^2f\,"(r_0)\right] \quad (24)$$

$$C_{144} = L\left[6.1585Z_m^2 + \frac{1}{9}(C_1 + 3B_1 - 3A_1) - 4.1681Zaf'(r_0) + 0.8407Za^2f\,"(r_0) + \nabla\left\{-3.3507Z_m^2 - \frac{2}{9}C_1 + 13.5486Zaf'(r_0) - 1.681Za^2f\,"(r_0)\right\} + \nabla^2\left\{-1.5637Z_m^2 + \frac{2}{3}(A_1 - B_1) + \frac{1}{9}C_1 - 5.3138Zaf'(r_0) + 2.9350Za^2f\,"(r_0)\right\}\right] \quad (25)$$

$$C_{166} = L\left[-2.1392Z_m^2 + \frac{1}{9}(C_1 - 6B_1 - 3A_1) + \frac{1}{8}(C_2 - 5B_2 - 3A_2) - (B_1 + B_2) - 4.1681Zaf'(r_0) + 0.8407Za^2f\,"(r_0) + \nabla\left\{-8.3768Z_m^2 + \frac{2}{3}(A_1 - B_1) - \frac{2}{9}C_1 + 13.5486Zaf'(r_0) - 1.681Za^2f\,"(r_0)\right\} + \nabla^2\left\{2.3527Z_m^2 + \frac{1}{9}C_1 - 5.3138Zaf'(r_0) + 2.9350Za^2f\,"(r_0)\right\}\right] \quad (26)$$

$$C_{456} = L\left[4.897Z_m^2 + \frac{1}{9}(C_1 - 6B_1 - 3A_1) - B_2 + \nabla\left\{-5.0261Z_m^2 - \frac{1}{9}C_1\right\} + \nabla^2\left\{7.0580Z_m^2 + \frac{1}{3}C_1\right\} + \nabla^3\left\{-4.8008Z_m^2 + \frac{1}{3}(A_1 - B_1) - \frac{1}{9}C_1\right\}\right] \quad (27)$$

where Z_m is the modified ionic charge defined earlier with $L = e^2/4a^4$ and

$$\nabla = \left[\frac{-7.53912Z(Z+8f(r_0))+(A_1-B_1)}{-3.141Z(Z+8f(r_0))+(A_1+2B_1)+21.765Zaf'(r_0)}\right] \quad (28)$$

and the expression for pressure derivatives of SOEC are-

$$\frac{dK'}{dP} = -(3\Omega)^{-1}[20.1788Z_m^2 - 3(A_1 + A_2) + 4(B_1 + B_2) + 3(C_1 + C_2) - 104.8433Zaf'(r_0) + 22.7008Za^2f\,"(r_0)] \quad (29)$$

$$\frac{dS'}{dP} = -(2\Omega)^{-1}\left[-11.5756Z_m^2 + 2(A_1 - 2B_1) + \frac{2A_2}{3} - \frac{7B_2}{2} + \frac{1}{4}\cdot C_2 + 37.5220Zaf'(r_0)\right] \quad (30)$$

$$\frac{dC_{44}'}{dP} = -(\Omega)^{-1}\left[\left\{0.4952Z_m^2 + \frac{1}{3}(A_1 - 4B_1 + C_1) + \frac{1}{2}\cdot A_2 - \frac{3}{2}\cdot B_2 - \frac{1}{4}\cdot C_2 + 4.9667Zaf'(r_0) + 2.522Za^2f\,"(r_0)\right\} + \nabla\left\{-17.5913Z_m^2 + A_1 - B_1 - \frac{2}{3}\cdot C_1 + 40.6461Zaf'(r_0) - 5.044Za^2f\,"(r_0)\right\} + \nabla^2\left\{3.1416Z_m^2 + \frac{2}{3}(A_1 - B_1) + \frac{1}{3}\cdot C_1 - 15.9412Zaf'(r_0) + 8.8052Za^2f\,"(r_0)\right\}\right] \quad (31)$$

where $K = \frac{C_{11}+2C_{12}}{3}$, $S = \frac{C_{11}-C_{22}}{2}$

and $\Omega = -5.0440Z_m^2 + (A_1 + A_2) - 2(B_1 + B_2) + 17.4730Zaf'(r_0)$

The values of *Ai*, *Bi* and *Ci* as defined by Sharma and Verma [28].

III. Computations

The model parameters {b, ρ and $f(r_0)$}, have been determined by using the expressions (19-21) and the equilibrium condition $\left(\frac{d\Phi(r)}{dr}\right)_{r_0=a\frac{\sqrt{3}}{2}} = 0$, with the inclusion of the van der Waal's interactions (VDWI) [equation (3)]. The values of the input data Lee [18], Jai Shankar et al. [30] and K. Kunc et al. [21] and model parameters have been shown in Table 1. The values of A_i, B_i, C_i have been calculated from the knowledge of b, ρ; the values of various order of derivatives are $f(r_0)$ and van der Waal's coupling coefficients [28]. The values of VDW coefficients used by us in the present study have been determined using the Slatre-Kirkwood

Variation (SKV) method [5], Lee [18] approach as suggested by Singh and Singh [29] and reported by Sharma and Verma [28]. Thus our model parameters are [b, ρ, $f(r_0)$, $r_0f'(r_0)$, A_{12}, A_{11}, A_{22}, B_{12}, B_{11}, B_{22}, d_1, d_2, Y_1 and Y_2]. The values of the van der Waal's coefficients (VDW) are shown in Table 2. Our model parameters of VTRSM have been used to compute the phonon spectra of ZnSe for the allowed 48 non-equivalent wave vectors in the first Brillouin zone. The frequencies along the symmetry directions have been plotted against the wave vector to obtain the phonon dispersion curves (PDCs). These curves have been compared with those measured by means of the coherent inelastic neutron scattering technique [19] in Figure 1 along with the DBM calculations of Kunc et al. [21]. Since the neutron scattering experiments provide us only very little data for the symmetry directions, we have also computed combined density of states (CDS) and the Debye temperatures variation for the complete description of the frequencies for the Brillouin zone.

The complete phonon spectra have been used to compute the combined density of states (CDS), $N(\upsilon_j+\upsilon_j')$ corresponding to the sum modes $(\upsilon_j+\upsilon_j')$ following procedure of Smart et al. [31]. A histogram between $N(\upsilon_j+\upsilon_j')$ and $(\upsilon_j+\upsilon_j')$ has been plotted and smoothed out as shown in Figure 2. These curves show well defined peaks which correspond to two-phonon Raman scattering and IR absorption spectra. These CDS peaks have been compared with the assignments calculated and shown in Table 3. The Debye temperatures variation for ZnSe measured from by Irwin and LaCombe [32] and those calculated by us using VTRSM has been compared in Figure 3. The calculated values of TOEC using equations (22-27) have been compared with calculated values of Anil et al. [33] and shown in Table 4. The pressure derivatives of SOEC have also been calculated and compared with those calculated by Khenata et al. [34] and Dinesh et al. [35] and measured by Lee [18] in Table 5.

IV. Results and Discussion

4.1 Phonon Dispersion Curves

From figure 1, our phonon dispersion curves for ZnSe agree well with measured data reported by Hennion et al. [31]. It is evident from PDCs that our predictions using present model (VTRSM) are better than those by using DBM [21]. Our model has successfully explained the dispersion of phonons along the three symmetry directions. From figure 1 and Table 6, it is clear that: there are deviations of 2.51% along LO(X), 2.28% along TO(X), 9.45% along LA(X), 13.33% along TA(X), 12.45% along LA(L) and 34.50% along TA(L) from experimental results. From DBM, deviations are 15.71% along TA(X), 12.85% along LA(L) and 35.08% along TA(L) while from VTRSM 2.38% along TA(X), 0.40% along LA(L) and 0.58% along TA(L). From Table 6 it is clear that VTRSM has very small deviation from experimental data. Our model VTRSM has 34.50% improvement over DBM due to inclusion of three body interactions (TBI) and VDWI coefficients. Therefore, our VTRSM model has better agreement with experimental data over DBM [21]. Furthermore, our results are very similar to those of recently reported by Tista Basak et al. [26].

4.2. Combined Density of States

The present model is capable to predict the two phonon Raman / IR spectra [19]. The results of these investigations for combined density states (CDS) peaks have been presented in Figure 2. The theoretical peaks are in good agreement with both observed Raman / IR spectra for ZnSe. The assignments made by the critical point analysis have been shown in Table 3. The interpretation of Raman / IR spectra achieved from both CDS approach and critical point analysis is quite satisfactory. This explains that there is an excellent agreement between experimental data and our theoretical results.

4.3. Third Order Elastic Constants (TOEC), Pressure Derivatives of Second Order Elastic Constants (SOEC)

Our calculations on TOEC have been reported in Table 4 and compared with measured data Prasad [36] on TOEC of ZnSe, theoretical results of Anil et al. [36]. Further, pressure derivatives of SOEC for ZnSe have also been compared with the calculated results of Dinesh et al. [35] and measured data of Lee et al. [18] as shown in Table 5. The results are in good agreement.

4.4. Debye Temperatures Variation

From figure 3, our study shows a better agreement with the measured data of Irwin and LaCombe [32] and the theoretical results reported by Hennion et al. [19] using rigid ion model (RIM). To conclude, we can say that our present model gives a better interpretation of the Debye temperatures variation for ZnSe.

V. Conclusion

The inclusion of van der Waal's interactions (VDWI) with TBI have influenced both the optical branches and the acoustic branches. Another striking feature of present model is noteworthy from the excellent reproduction of almost all branches. Hence the prediction of phonon dispersion curves (PDC) for

ZnSe using VTRSM may be considered more satisfactory than from other models DBM [21]. The basic aim of the study of two phonon Raman / IR spectra is to correlate the neutron scattering and optical measured data of ZnSe. In this paper, we have systematically reported phonon dispersion curves, combined density of states, Debye temperatures variation and a part of harmonic and anharmonic properties of ZnSe. On the basis of overall discussion, it is concluded that our van der Waal's three body rigid shell model (VTRSM) is adequately capable of describing the crystal dynamics of zinc selenide. This model has also been applied equally well to study the crystal dynamics of other compound of this group ZnS and has been accepted for publication [40] and is in press. Its application to ZnTe is ready for communication. Our work gets strong support from paper of Mishra and Upadhyaya [41].

Acknowledgements

The authors are thankful to Computer Center, BHU, Varanasi, India for providing computational assistance. One of us Jay Prakash Dubey is also thankful to Dr. Devendra Pathak, vice chancellor, Dr. K. N. Modi University Newai, Rajasthan, India for encouragement.

References

[1] Born M. and Mayer J. E. Z. Phys. 75, 1 (1932).
[2] Tosi M. P. and Fumi F. G. J. Phys. Chem. Solids. 23, 359 (1962).
[3] Hafemeister D. W. and Flygare W. H. J. Chem. Phys. 43, 795 (1965).
[4] Singh R . K . Physics Reports (Netherlands) 85, 259 (1982).
[5] Slater J. C. and Kirkwood J. G. Phys. Rev. 37, 682 (1931).
[6] San-Miguel A., Polian A., Gauthier M. and Itie J. P. Phys. Rev. B 48, 8683 (1993).
[7] Nelmes R . J., McMahon M. I., Wright N. G. and Allan D. R. Phys. Rev. Lett. 73, 1805 (1994).
[8] McMahon M. I. and Nelmes R. J. J. Phys. Chem. Solids 56, 485 (1995).
[9] Cote M., Zakharov O., Rubio A. and Cohen M. L. Phys. Rev. B 55, 13025 (1997).
[10] Qteish A. and Munoz A. J. Phys. Condens. Matter 12, 1705 (2000).
[11] Pellicer-Porres J., Segura A., Munoz V., Zuniga J., Itie J. P., Polian A. and Munsch P. Phys. Rev. B 65, 012109 (2001).
[12] Gangadharan R., Jayalakshami V., Kalaiselvi J., Mohan S., Murugan R. and Palanivel B. J. Alloys Compounds 359, 22 (2003).
[13] Lopez- Solano J., Mujica A., Rodriguez - Hernandez P. and Munoz A. Phys. Status Solidi (b) 235, 452 (2003).
[14] Mujica A., Rubio A., Munoz A. and Needs R . J. Rev. Mod. Phys. 75, 863 (2003).
[15] Ovsyannikov S. V. and Shchennikov V. V. Solid State Commun. 132 , 333 (2004).
[16] Cui S., Hu H., Feng W., Chen X. and Feng Z. J. Alloys compounds 472 , 294 (2009).
[17] Berlin Court. D., Jaffe H., Shiozawa L. R. Phys. Rev. 129, 1009 (1963).
[18] Lee B. H. J. Appl. Phys. 41, 2988 (1970).
[19] Hennion B., Moussa F., Pepy G. and Kunc. K. Phys. Lett. 36, 376 (1971).
[20] Hodgins C. G. and Irwin J. C. Phys. Status Solidi A 28, 647 (1975).
[21] Kunc K., Balkanski M. and Nusimovici M. A. Phys. Status Solidi (b) 71, 341(1975) (b) 72**,** 229 (1975) (b) 72, 220 (1975).
[22] Talwar D. N., Vandevyver M., Kunc. K. and Zigone M. Phys. Rev. B 24, 9052 (1981).
[23] Rajput B. D., Browne D. A. Phys. Rev. B 53, 9052 (1996).
[24] Sharma P. Ind. Jour. Res. 2, 100 (2013).
[25] Wang H. Y., Cao J., Huang X. Y. and Huang J. M. Condens. Matter Phys. 15, 1 (2012).
[26] Basak Tista, Rao N. Mala, Gupta M. K. and Chaplot S. L. J. Phys. Condens. Matter 24, 115401 (2012).
[27] Singh R. K. and Khare P. J. Phys. Soc. Japan 51, 141 (1982).
[28] Sharma U. C. and Verma M. P. Phys. Status Solidi (b) 102, 487 (1980).
[29] Singh R. K. and Singh S. Phys. Status Solidi (b) 140, 407 (1987).
[30] Shankar Jai, Sharma J. C. and Sharma D. P. Ind. J. Pure Appl. Phys. 5, 811 (1977).
[31] Smart C., Wilkinson G. R. , Karo A. M. and Lattice Dynamics, edited by Wallis R. F. (1965) (Pergamon Press oxford)
[32] Irwin J. C. and LaCombe J. J. Appl. Phys. 45, 567 (1974).
[33] Anil T. V., Menon C. S., Kumar Krishna K Shree Chandran and Jaya K. P. J. Phys., Chem. Sol. 65, 1053 (2004).
[34] Khenata R., Bouhemadou A., Sahnoun M., Reshak Ali H., Baltache H. and Rabah M. Comp. Mat. Sci. 38, 29 (2006).
[35] Varshney Dinesh, Sharma P., Kaurav N. and Singh R. K. Bull. Mat. Sci. 28, 651 (2005).
[36] Prasad O. H. PhD Thesis, Osmania University, Hyderabad, India (1978).
[37] Irwin J. C. and LaCombey Cand. J. Phys. 48, 2499 (1970).
[38] Nilsen W. G. Phys. Rev. 182, 838 (1969).
[39] Mitra S. S. Phys. Rev. 132, 986 (1963).
[40] Dubey Jay Prakash, Tiwari Raj Kishore, Upadhyaya Kripa Shankar and Pandey Pramod Kumar, Turk. J. Phys. (2015 in press)
[41] Mishra K. K. and Upadhyaya K. S. Int. Jour. Sci. Engg. Res. 3, 1388 (2012).

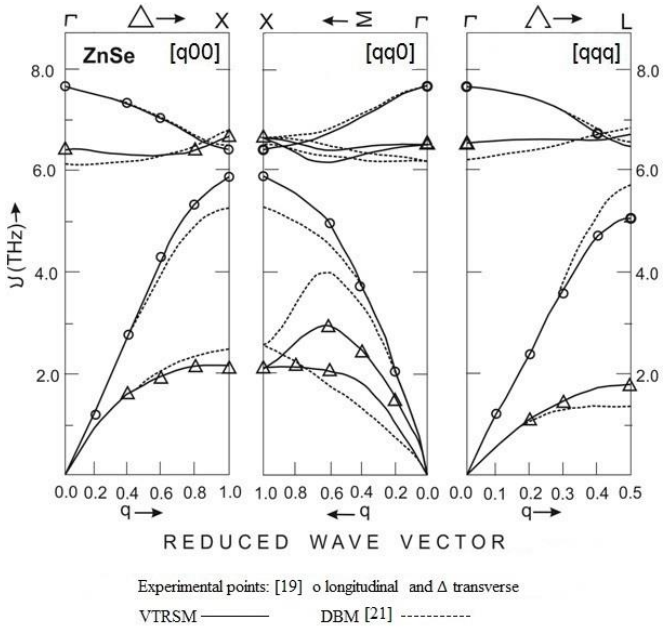

Figure 1: Phonon dispersion curves for ZnSe

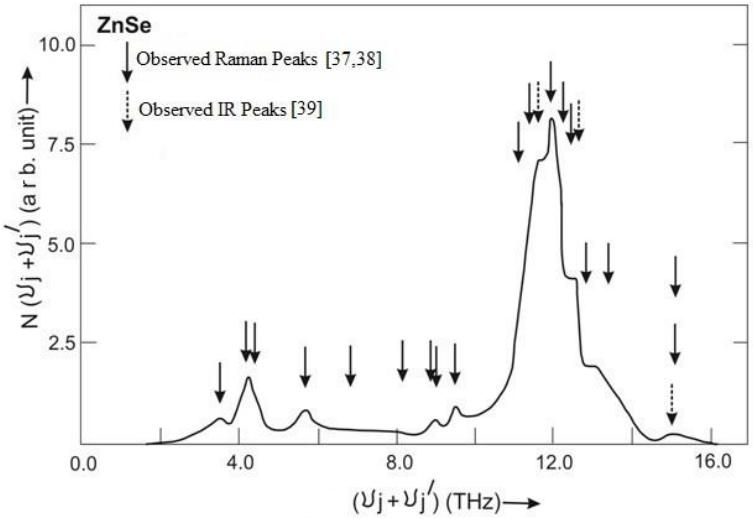

Figure 2: Combined density of states curve for ZnSe

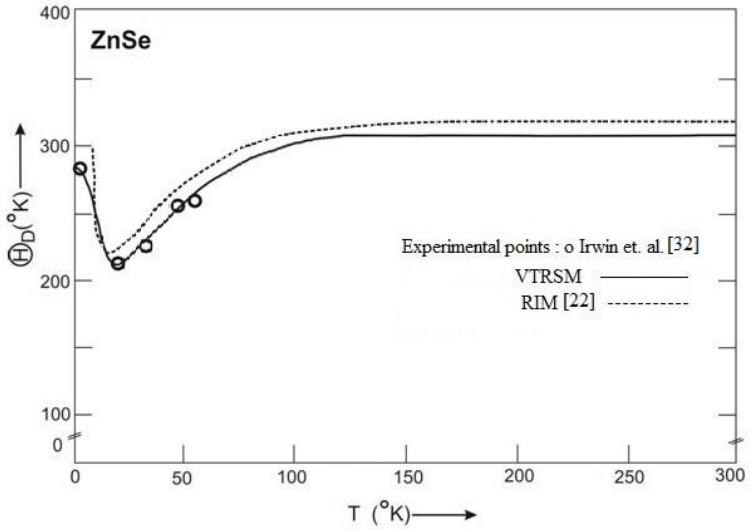

Figure 3: Debye characteristics temperatures Θ_D (°K) as a function of temperature T for ZnSe

Table 1. Input data and model parameters for ZnSe [C_{ij} and B (in 10^{11} dyne/cm^2), υ (in THz), r_0 (in 10^{-8} cm), α_i (in 10^{-24} cm^3), b (in 10^{-12} erg), ρ (in 10^{-8} cm)]

Input Data		Model Parameters	
Properties	Values	Parameters	Values
C_{11}	8.59[a]	b	1.6000
C_{12}	5.06[a]	ρ	0.4930
C_{44}	4.06[a]	$f(r_0)$	-0.0274
B	6.24[b]	$r_0 f'(r_0)$	0.1322
r_0	2.45[b]	A_{12}	16.2445
$\nu_{LO}(\Gamma)$	7.59[c]	B_{12}	-5.4020
$\nu_{TO}(\Gamma)$	6.39[c]	A_{11}	107.8440
$\nu_{LO}(L)$	6.40*	B_{11}	-22.2153
$\nu_{TO}(L)$	6.60*	A_{22}	-4.2166
$\nu_{LA}(L)$	4.98[c]	B_{22}	-6.8826
$\nu_{TA}(L)$	1.71[c]	d_1	0.2963
α_1	1.08[d]	d_2	2.9222
α_2	5.94[d]	Y_1	-2.3148
ε_0	5.90[e]	Y_2	-1.2909

*Extrapolated values from [19].

[a]-(B. H. Lee [18]); [b]- (D. Berlin Court et al. [17]); [c]–(Hennion et al. [19]); [d]- (Jai Shankar et al. [30]) and [e]- (K. Kunc. et al. [21]);

Table 2. van der Waal's interaction coefficients for ZnSe (C_{ij} and C in units of 10^{-60} erg cm^6 and d_{ij} and D in units of 10^{-76} erg cm^8)

Parameters	Numerical Values
C_{+-}	213
C_{++}	66
C_{--}	844
d_{+-}	170
d_{++}	23
d_{--}	662
C	1275
D	725

Table 3. Assignments for the observed peak positions in combined density of states in terms of selected phonon frequencies at Γ, X and L critical points for ZnSe

CDS Peaks (cm^{-1})	Raman Active			Infra-Red Active		
	Observed Raman Peaks (cm^{-1}) [37, 38]	Present Study		Observed IR Peaks (cm^{-1}) [39]	Present Study	
		Values (cm^{-1})	Assignments		Values (cm^{-1})	Assignments
.....	.....	112	2TA(L)	.....	.....	.....
117	117	115	$TO_1+TA_1(\Delta)$	.....	.....	.....
139	139, 146[a]	138	LO-TA (X)	.....	.....	.....
.....	.....	142	2TA(X)	.....	.....	.....
189	189	192	$2TA_1(\Delta)$	.....	192	$2TA_1(\Delta)$
.....	228	222	LA+TA (L)	.....	.....	.....
.....	.....	259	$LA+TA_1(\Delta)$	.....	.....	.....
.....	270	264	LA+TA (X)	.....	269	LO+TA(L)
.....	.....	.....	.....	.....	276	TO+TA(L)
.....	296, 297[a]	291	TO+TA(X)	.....	.....	.....
299	.....	307	$TO_1+TA_1(\Delta)$	.....	307	$TO_1+TA_1(\Delta)$
317	317	319	$LO+TA_1(\Delta)$	.....	319	$LO+TA_1(\Delta)$
.....	368	.....	2LA(L)	.....	.....	.....
370	381	374	$TO_1+LA(\Delta)$	371	374	$TO_1+LA(\Delta)$
.....	.....	.....	.....	.....	379	LO+LA(L)
396	396	386	2LA(X)	.....	.....	.....
.....	.....	402	LO+LA (X)	.....	.....	.....
.....	407	406	2TO(Γ)	.....	.....	.....
.....	414	413	TO+LA(X)	.....	.....	.....
420	.....	422	$2TO_1(\Delta)$	420	422	$2TO_1(\Delta)$
432	431	433	LO+TO(L)	.....	.....	.....
.....	.....	434	$LO+TO_1(\Delta)$	.....	434	$LO+TO_1(\Delta)$
.....	448	446	$2LO(\Delta)$	.....	446	$2LO(\Delta)$
503	503, 504[a]	506	2LO(Γ)	501	.....	.....

Reference [a]–[38]

Table 4. Third order elastic constants (in the unit of 10^{11}dyne/cm^2) for ZnSe

Property	Present Study	Experimental Results [36]*	Other Theoretical Results [33]
C_{111}	- 92.5	-82.7	-52.0
C_{112}	- 10.0	-13.6	-26.2
C_{123}	-45.6	-55.1	-0.04
C_{144}	-18.0	-22.2	-0.34
C_{166}	- 29.1	-26.5	-25.6
C_{456}	-25.6	-27.8	-0.08

*Results noted for comparison from Anil et al. [21]

Table 5. Values of pressure derivatives of SOEC (in dimensionless) for ZnSe

Properties	Values		
	Present Study	Experimental [18]	Other [35]
dK'/dP	5.12	4.77	4.86
dS'/dP	-0.19	-0.12	-0.39
dC'$_{44}$/dP	0.52	0.43	1.13

Table 6. Comparison of frequencies from various sources (X and L points) for ZnSe

Points	Branches (THz)	Expt. [19]	DBM [21]			Present Study			% Improvement Over DBM (a ~ b)
			Value	(±) Deviation	% (a)	Value	(±) Deviation	% (b)	
X (100)	LO	6.39	6.56	0.17	2.66	6.38	0.01	0.15	2.51
	TO	6.59	6.75	0.16	2.43	6.60	0.01	0.15	2.28
	LA	5.82	5.25	0.57	9.79	5.80	0.02	0.34	9.45
	TA	2.10	2.43	0.33	15.71	2.15	0.05	2.38	13.33
L (.5.5.5)	LO	.....	6.37	6.37	.....	6.40	.....	.....	.....
	TO	.....	6.56	6.56	.....	6.60	.....	.....	.....
	LA	4.98	5.62	0.64	12.85	5.00	0.02	0.40	12.45
	TA	1.71	1.11	0.60	35.08	1.70	0.01	0.58	34.50